

See discussions, stats, and author profiles for this publication at: <https://www.researchgate.net/publication/5995589>

Rate Constants of Hydroperoxyl Radical Addition to Cyclic Nitrones: A DFT Study

ARTICLE *in* THE JOURNAL OF PHYSICAL CHEMISTRY A · NOVEMBER 2007

Impact Factor: 2.69 · DOI: 10.1021/jp073615s · Source: PubMed

CITATIONS

22

READS

28

4 AUTHORS, INCLUDING:



Frederick A. Villamena

The Ohio State University

88 PUBLICATIONS 1,677 CITATIONS

SEE PROFILE

Published in final edited form as:

J Phys Chem A. 2007 October 4; 111(39): 9995–10001. doi:10.1021/jp073615s.

Rate Constants of Hydroperoxyl Radical Addition to Cyclic Nitrones: A DFT Study

Frederick A. Villamena^{1,2,*}, John K. Merle⁴, Christopher M. Hadad^{4,*}, and Jay L. Zweier^{2,3}

¹Department of Pharmacology, The Ohio State University, Columbus, Ohio, USA 43210.

²Center for Biomedical EPR Spectroscopy and Imaging, The Davis Heart and Lung Research Institute, The Ohio State University, Columbus, Ohio, USA 43210.

³Division of Cardiovascular Medicine, Department of Internal Medicine, College of Medicine, The Ohio State University, Columbus, Ohio, USA 43210.

⁴Department of Chemistry, The Ohio State University, Columbus, Ohio, USA 43210.

Abstract

Nitrones are potential synthetic antioxidants against the reduction of radical-mediated oxidative damage in cells, and as analytical reagent for the identification of HO_2^\bullet and other such transient species. In this work, the PCM/B3LYP/6–31+G(d,p)//B3LYP/6–31G(d) and PCM/mPW1K/6–31+G(d,p) density functional theory (DFT) methods were employed to predict the reactivity of HO_2^\bullet with various functionalized nitrones as spin traps. The calculated second-order rate constants and free energies of reaction at both levels of theory were in the range of 10^0 – $10^3 \text{ M}^{-1} \text{ s}^{-1}$ and 1 to $-12 \text{ kcal mol}^{-1}$, respectively, and the rate constants for some nitrones are on the same order of magnitude as those observed experimentally. The trend in HO_2^\bullet reactivity to nitrones could not be explained solely on the basis of the relationship of the theoretical positive charge densities on the nitronyl-C, with their respective ionization potentials, electron affinities, rate constants, or free energies of reaction. However, various modes of intramolecular H-bonding interaction were observed at the transition state (TS) structures of HO_2^\bullet addition to nitrones. The presence of intramolecular H-bonding interactions in the transition states were predicted and may play a significant role towards a facile addition of HO_2^\bullet to nitrones. In general, HO_2^\bullet addition to ethoxycarbonyl- and spiroactam-substituted nitrones, as well as those nitrones without electron-withdrawing substituents, such as 5,5-dimethyl-pyrroline *N*-oxide (DMPO) and 5-spirocyclopentyl-pyrroline *N*-oxide (CPPO), are most preferred compared to the methylcarbamoyl-substituted nitrones. This study suggests that the use of specific spin traps for efficient trapping of HO_2^\bullet could pave the way toward improved radical detection and antioxidant protection.

1. Introduction

Superoxide radical anion ($\text{O}_2^{\bullet-}$) has attracted considerable attention over the last 3 decades because it has been shown that $\text{O}_2^{\bullet-}$ and $\text{O}_2^{\bullet-}$ -derived reactive oxygen species (ROS), such as HO^\bullet , HO_2^\bullet , RO_2^\bullet , RO^\bullet , $\text{CO}_3^{\bullet-}$ and $\text{CO}_2^{\bullet-}$; as well as non-radicals, such as H_2O_2 , HOCl and ROOH , in unregulated concentrations are critical mediators of pathogenesis for various diseases.¹ The formation of hydroperoxyl radical (HO_2^\bullet) from $\text{O}_2^{\bullet-}$ is relevant in both chemical

* Correspondence to: Frederick.Villamena@osumc.edu, Fax: (614)–688–0999. hadad.1@osu.edu, Fax: (614)–292–1685; Jay.Zweier@osumc.edu, Fax: (614)–247–7799..

Supporting Information Available. Energies, enthalpies, and free energies for all spin traps and their corresponding spin adducts are available as supporting information. This information is available free of charge at <http://pubs.acs.org>

and biological systems. For example, in simple chemical systems, HO_2^\bullet has been shown to be produced from O_2^\bullet by a proton-transfer reaction from phenol or one-electron reduction of O_2 in the presence of HClO_4 .² Furthermore, the presence of a small equilibrium concentration of HO_2^\bullet in neutral pH (pK_a for HO_2^\bullet is 4.8³ or 4.4⁴) can contribute to O_2^\bullet instability via a dismutation reaction with a reaction rate of $k = 9.7 \times 10^7 \text{ M}^{-1} \text{ s}^{-1}$.⁵

The generation of HO_2^\bullet is relevant in the initiation of lipid peroxidation in cellular systems.⁶ *In vivo* rat heart studies show that the ischemic period (a condition by which the tissues or organs are deprived of blood flow) and immediate reperfusion have enhanced oxygen radical production^{7,8} and are accompanied by ischemia-induced acidosis.⁹ These two processes by which O_2^\bullet can be generated under acidic conditions may have detrimental consequences, resulting in oxidative damage to cellular systems as HO_2^\bullet is a stronger oxidizer than O_2^\bullet ($E^\circ = 1.06$ and 0.94 V , respectively).⁵

Spin trapping¹⁰ with cyclic nitrones in combination with electron paramagnetic resonance (EPR) spectroscopy has been the method of choice for detection of ROS, particularly for O_2^\bullet in biological systems. However, it is not clear if the resulting nitron-O₂H adduct observed by EPR is initially formed from spin trapping of O_2^\bullet or HO_2^\bullet .^{11,12} Therefore, a comparison of the second-order rate constants for the direct addition of HO_2^\bullet and O_2^\bullet to cyclic nitrones in solution can provide valuable information on to the nature of the radical species formed, and hence, be useful in elucidating mechanisms which may involve radical generation in cellular systems.

Nitrones have also been employed as intermediates in the synthesis of natural products¹³ and therapeutic agents.¹⁴⁻¹⁶ For example, the linear-nitron, disodium-[(*tert*-butylimino)-methyl] benzene-1,3-disulfonate *N*-oxide (NXY-059) is in clinical trials in the USA as a potential therapeutic for neurodegenerative disease.¹⁷ Moreover, the cyclic nitrones, 5,5-dimethylpyrroline *N*-oxide (DMPO) and 5-(diethoxyphosphoryl)-5-methyl-1-pyrroline *N*-oxide (DEPMPO) (see Chart 1) has been shown to exhibit cardioprotective properties upon its perfusion in a rat's heart after ischemia.¹⁸ However, questions arise regarding the mechanism providing the antioxidant property of nitrones,^{15,19} since for example, DMPO reactivity with O_2^\bullet ² at physiological pH (~ 7) is slow, $k = \sim 10 \text{ M}^{-1} \text{ s}^{-1}$ and at pH 5, the rate is on the order of $10^3 \text{ M}^{-1} \text{ s}^{-1}$.²⁰ Therefore, the significantly higher rate of spin trapping of HO_2^\bullet , as compared to O_2^\bullet , with DMPO may partly account for the antioxidant properties of nitrones. However, other mechanisms for the protective property of nitrones against oxidants have also been proposed.^{15,16} Boyd and Boyd²¹ reported the energetics of spin trapping of HO_2^\bullet by a prototype nitron, $\text{H}_2\text{C}=\text{NHO}$, with $\Delta E_{\text{MP2}} = -141 \text{ kJ/mol}$ (-33.7 kcal/mol) at the MP2/6-31G(d,p)//HF/6-31G(d). Moreover, we previously reported theoretical free energies for O_2^\bullet and HO_2^\bullet addition to nitrones that have average $\Delta G_{\text{rxn, aq, 298K}} = 10.0 \pm 3.0$ and $-7.0 \pm 1.6 \text{ kcal/mol}$, respectively.²²

Correctly interpreting the nature of radical species formed in solution is important to accurately elucidate the mechanism(s) for radical production in chemical²³ and biological systems.^{8,24} In a separate study,²⁵ we predicted, and experimentally determined, the bimolecular rate constants for O_2^\bullet addition to various nitron spin traps. However, this work will focus on the prediction of second-order rate constants for HO_2^\bullet addition to various cyclic nitrones. So far, most of our theoretical work has focused on the prediction of thermodynamic parameters for the spin-trapping of HO_2^\bullet .²² Although thermodynamic data provide insight into the favorability for formation of certain products, they provide no direct information in order to predict the relative rates by which spin trapping occurs. In this study, the second-order rate constants (k_2) in solution for HO_2^\bullet addition to a variety of important nitrones were theoretically predicted and found to agree well with available experimental values.

II. Computational Methods

General Procedure

Gaussian 03 (Revision B.05) was used for all calculations.²⁶ Hybrid density functional theory²⁷ was employed to obtain optimized geometries and vibrational frequencies for all stationary points at the B3LYP/6-31G(d) and mPW1K/6-31+G(d,p) levels.²⁸ The mPW1K calculations were initiated by requesting iop (5/45=10000428,5/46=05720572,5/47=10001000) in the route card. The mPW1K method has been shown by Truhlar and co-workers to be very effective for determining transition state (TS) structures and barrier heights for H-atom transfer reactions.²⁹ Single-point energies on the optimized B3LYP/6-31G(d) geometries were obtained at the B3LYP/6-31+G(d,p) level. The effect of solvation was investigated via single-point energy calculations at the B3LYP/6-31+G(d,p) level using the polarizable continuum model (PCM) to represent water.³⁰ Stationary points, as minima for both the nitron spin traps and their respective HO₂[•] adducts, were determined to have zero imaginary vibrational frequencies as derived from a harmonic vibrational frequency analysis at the level at which the stationary points were optimized. Scaling factors of 0.9806³¹ and 0.9515³² were used for zero-point vibrational energy (ZPE) corrections for the B3LYP and mPW1K geometries, respectively. Free energies were obtained from the calculated thermal and entropic corrections at 298 K using the unscaled vibrational frequencies. For the minima, spin contamination values for the radical adducts are negligible, i.e., $0.75 < \langle S^2 \rangle < 0.80$ (see Tables S2-S7). Spin densities (populations) and charge densities were obtained from a natural population analysis (NPA) of the electronic wavefunctions at the PCM/B3LYP/6-31+G(d,p)/B3LYP/6-31G(d) and PCM/mPW1K/6-31+G(d,p) levels.³³

Initial nitron and spin-adduct structures for transition state (TS) searches were chosen based on the most stable conformer/configuration resulting from the PCM aqueous phase energies. Transition states (TS) were confirmed to have one imaginary vibrational frequency, and furthermore, shown to be connected to the desired reactant and product by displacement along the normal coordinate (typically 10%) for the imaginary vibrational frequency in the positive and negative directions followed by careful minimization using opt = calcfc. Hence, all HO₂[•] adduct structures reported here are the result of minimizing the energy of the displaced TS structures.

To predict rate constants, we examined the potential energy surfaces and located maxima, and we have been successful in locating a variety of TS's for such reactions in the recent past.^{22, 25,34} The $\langle S^2 \rangle$ values for the TS have typically shown minimal spin contamination, i.e., $0.81 < \langle S^2 \rangle < 0.82$. Conventional transition state theory (TST) was utilized to estimate the rates for spin-adduct formation at 298 K.³⁵ The conventional TST rate equation in the thermodynamic formulation as a function of temperature is as follows:

$$k(T)_{TST} = \Gamma(T) \frac{k_B T}{h} \exp\left(-\Delta G_0^\ddagger / k_B T\right) \quad (1)$$

In Equation 1, T is the absolute temperature, h is Planck's constant, k_B is Boltzmann constant, and ΔG_0^\ddagger is the free energy barrier height relative to reactants at infinite separation. The temperature dependent factor $\Gamma(T)$ represents quantum mechanical tunneling and is accounted for by the Wigner approximation:³⁶

$$\Gamma(T) = 1 + \left(\frac{1}{24}\right) \left[1.44 \frac{\nu_i}{T}\right]^2 \quad (2)$$

in which ν_i is the imaginary vibrational frequency representing the TS barrier's curvature.

III. Results and Discussion

A. Nitrones and Hydroperoxyl Adducts

Selected bond distances for the B3LYP/6–31G(d) optimized geometries of the nitrone spin traps and their corresponding HO₂[•] adducts are shown in Table S1 of the supporting information. All of the relevant bond distances for the nitrone and nitroxyl moieties as well as the various electron-withdrawing substituents are in good agreement with reported experimental X-ray crystallographic bond lengths for related compounds.³⁷

We previously²⁵ established, by a computational approach, that in aqueous solution, the amide functionality of AMPO, MAMPO, and DiMAPO (Chart 1) are predominantly in the amide form (or lactam form for TAMPO), rather than in the respective imidic acid (or lactim) form. Spin-adduct structures have O–O bond distances from 1.41–1.42 Å in all of the HO₂[•] adducts. The C_{ring}–O₂H bond distances are in the 1.37–1.43 Å range, similar to that observed experimentally for cyclic hydroperoxides (~1.46 Å).³⁸ The conformations for various HO₂[•] adducts with nitrones obtained at the B3LYP/6–31G(d) level correlate well with those at the mPW1K/6–31+G(d,p) level of theory (Table 1), with the exception of CPCOMPO–O₂H in which the predicted O–O–C–N dihedral angle is smaller (56.4°) at the B3LYP/6–31G(d) level as compared to mPW1K/6–31+G(d,p) (286.6°). An O₂H---O–N H-bonding interaction was observed for the HO₂[•] adducts of DiMAMPO, DiMAPO, DEPMPO, DMPO, TFMPO, MSMPO, CPPO, and EMPO, with an H---O bond distances ranging from 2.04 to 3.09 Å. An O₂H---O=C H-bonding interaction was predicted for DEPO, CPCOMPO, and TAMPO with H---O distances between 1.84 and 1.99 Å, while an O₂H---NR₂ interaction was predicted for AMPO, MAMPO, and EMAPO with H---N distances of 2.30 to 2.42 Å. (See Figure S1 of the supplementary information for the mPW1K/6–31+G(d,p) structural parameters.)

Figure 1 shows the most favored diastereomer (2*S*,5*R*) for the EMAPO–O₂H adduct in which the amido group is *trans* to the HO₂ moiety. The preferred (2*S*,5*R*) isomer for EMAPO–O₂H exhibits two intramolecular H-bond interactions, (i.e., N–O---H–N and OOH---O–N) which are *trans* to each other and are more stable than the (2*R*,5*R*) isomer by –0.6 kcal/mol.

B. Transition State Structures

The TS structures for HO₂[•] addition to the nitrones were calculated, and each stationary point gave a single imaginary vibrational frequency corresponding to motion along the C₂–O₂H bond axis (Table 2). The TSs for HO₂[•] addition have imaginary vibrational frequencies ranging from 323*i* to 517*i* cm^{–1} at the B3LYP/6–31G(d) level and 312*i* to 411*i* cm^{–1} at the mPW1K/6–31+G(d,p) level (Table 2).

The transition states have a narrow range of C₂---O₂H distances, ranging from 2.00–2.12 Å and 2.10–2.15 Å at the B3LYP/6–31G(d) and mPW1K/6–31+G(d,p) levels, respectively. These calculated C₂---O₂H distances are intermediate between the distances calculated for the complexed form and the final adduct as a product (Table 2). The TS structures for HO₂[•] addition have average sums of the bond angles around the C₂ carbon of 356.6 ± 1.0°; intermediate to those predicted for the nitrones (360.0 ± 0.1°) and their respective HO₂[•] adduct products (328.1 ± 1.2°). In light of Hammond's postulate, the sums of the bond angles suggest that the TS for HO₂[•] addition is early on the reaction coordinate; i.e., the TS structures are closer to the reactants.

Table 3 shows the spin density distribution for the various TS structures for HO₂[•] addition at the B3LYP/6–31+G(d,p)//B3LYP/6–31G(d) and they are all very similar. The average spin densities (populations) on the nitronyl–N, nitronyl–O, hydroperoxyl–β–O, and hydroperoxyl–γ–O atoms are 0.18 ± 0.03, 0.30 ± 0.03, 0.52 ± 0.03, and 0.17 ± 0.02 e, respectively. The same trend has been observed at the mPW1K/6–31+G(d,p) level (Table S8). The calculated spin

densities for the HO₂[•] atoms are 0.73 e for the distal O and 0.27 e on the proximal O relative to H, indicating that some electron transfer occurs from the HO₂[•] to the nitron in the TS. We note that this behavior is contrary to the reaction of hydroxyl radical with electron-rich aromatic rings for which electron transfer from the aromatic unit is transferred to the hydroxyl moiety.³⁹ The HO₂[•] adduct structures show almost complete spin-population transfer to the nitroxyl moiety with spin densities of 0.43 e and 0.52 e on the nitroxyl N and O, respectively.

The OOH---O=C, OOH---NR₂, and OOH---O-N H-bond distances in the transition states are very similar to H-bond distances observed in their respective product structures with deviations of 0.1–0.3 Å (Figure S1). These predicted interactions play a significant role in stabilizing the TS structures, and hence, in the facile formation of the adducts as products. All predicted TS H-bonding interactions are present for both B3LYP/6–31G(d) and mPW1K/6–31+G(d,p) optimized structures.

C. Calculated Bimolecular Rate Constants

In our previously studies,^{11,40} we showed that the direct addition of HO₂[•] to DMPO is one of the two possible mechanisms for the formation of DMPO-O₂H in aqueous solution with O₂^{•-} addition followed by proton transfer being the other. This reaction is relevant since the generation of O₂^{•-} in acidic condition can favor direct radical addition of HO₂[•] instead of O₂^{•-} to DMPO. The free energies for O₂^{•-} protonation by hydronium ion in an aqueous medium is highly exoergic; $\Delta G_{\text{rxn-1,aq}} = -41.1$ and -40.5 kcal/mol at the PCM/mPW1K/6–31+G(d,p) and PCM/B3LYP/6–31+G(d,p)//B3LYP/6–31G(d) levels, respectively (see Table 4).

Reactions for HO₂[•] addition to nitrones are exoergic with $\Delta G_{\text{rxn-2,aq}}$ (Table 4) values that range from -5.1 to -11.5 kcal/mol, while O₂^{•-} additions to nitrones are endoergic with $\Delta G_{\text{aq}} = 0.7$ to 8.3 kcal/mol at the PCM/mPW1K/6–31+G(d,p) level.²⁵ These free energies of reaction are consistent with the experimental reduction potentials of $E^0 = 1.06$ and 0.94 V for HO₂[•] and O₂^{•-}, respectively.⁴¹ The free energies of reaction for HO₂[•] reactions with nitrones follow the order of increasing (more positive) ΔG_{rxn} (in kcal/mol): MSMPO (-10.2) > DEPO (-10.1) > EMPO (-9.5) > TFMPO (-9.4) > DiMAMPO (-8.9) > CPCOMPO (-8.7) > DEPMPO (-8.6) > TAMPO = CPPO (-8.5) > DMPO (-8.2) > EMAPO trans addition to amide group (-8.0) > DiMAPO (-5.6) > AMPO (-5.5) > MAMPO = EMAPO cis addition to amide group (5.1) and the *N*-monoalkylamide substituted nitrones MAMPO, DiMAPO, and EMAPO (Table 4). In contrast to the predicted thermodynamics for the O₂^{•-} additions to amide-substituted nitrones which is the most favorable, the HO₂[•] additions to *N*-monoalkylamide substituted nitrones were not the most thermodynamically favored.²⁵

At the PCM/mPW1K/6–31+G(d,p)//mPW1K/6–31+G(d,p) level, the calculated rate constants, $k_{\text{rxn-2}}$, for HO₂[•] addition to nitrones are the greatest for DEPO ($k_{\text{rxn-2}} = 3.0 \times 10^3 \text{ M}^{-1} \text{ s}^{-1}$) followed by TAMPO ($k_{\text{rxn-2}} = 1.9 \times 10^3 \text{ M}^{-1} \text{ s}^{-1}$), trans addition to the amide moiety of EMAPO ($k_{\text{rxn-2}} = 1.4 \times 10^3 \text{ M}^{-1} \text{ s}^{-1}$), EMPO ($k_{\text{rxn-2}} = 1.5 \times 10^3 \text{ M}^{-1} \text{ s}^{-1}$), CPPO ($k_{\text{rxn-2}} = 1.1 \times 10^3 \text{ M}^{-1} \text{ s}^{-1}$) and DMPO ($k_{\text{rxn-2}} = 1.0 \times 10^3 \text{ M}^{-1} \text{ s}^{-1}$). The TFMPO, DEPMPO and MSMPO nitrones have intermediate rate constants with values $k_{\text{rxn-2}} = 276.0$, 125.8 and $105.9 \text{ M}^{-1} \text{ s}^{-1}$, respectively. The nitrones that have the smallest rate constants for HO₂[•] addition are the amide-nitrones, i.e., AMPO, MAMPO, DiMAMPO, DiMAPO, and EMAPO (where the HO₂[•] addition is *cis* to the amide group), as well as CPCOMPO where the rate constants are in the range 1.3 to $61.9 \text{ M}^{-1} \text{ s}^{-1}$ (see Table 4). The same qualitative trend is predicted at the PCM/B3LYP/6–31+G(d,p)//B3LYP/6–31G(d) level, with the exception of DEPMPO.

The electronic and thermodynamic parameters including the C₂ charge densities, rate constants, free energies, electron affinities and ionization potentials calculated at the PCM/mPW1K/6–31+G(d,p)//mPW1K/6–31+G(d,p) level correlate well with those calculated at the PCM/B3LYP/6–31+G(d,p)//B3LYP/6–31G(d) level of theory as shown in the Figure S2 of

the supplementary information. However, the preference for HO_2^\bullet addition to certain nitrones does not follow the same trend observed for $\text{O}_2^{\bullet-}$ addition that we reported recently²⁵ in which we demonstrated a dependence of $k_{\text{rxn-2}}$ and $\Delta G_{\text{rxn-2}}$ on the C_2 charge density of the nitron. The PCM/mPW1K/6-31+G(d,p)//mPW1K/6-31+G(d,p) $k_{\text{rxn-2}}$ and $\Delta G_{\text{rxn-2}}$ values for HO_2^\bullet addition to nitrones give a poor correlation with nitron C_2 charge densities (see Figures S3a and S3b). Poor correlation also resulted from the PCM/B3LYP/6-31+G(d,p)//B3LYP/6-31G(d) values (see Figure S4a and S4b). The poor correlation between the C_2 charge densities and the favorability of HO_2^\bullet addition to nitrones suggests that electrostatic effects play a minor role in these HO_2^\bullet reactions.

In general, the magnitude of $k_{\text{rxn-2}}$, which is in the order of 1 to $10^3 \text{ M}^{-1} \text{ s}^{-1}$, agrees well with the bimolecular rate constants observed experimentally in acidic solutions for the spin trapping of $\text{O}_2^{\bullet-}$ by nitrones.^{20,42} However, a plausible explanation for the difference in nucleophilicity between HO_2^\bullet and $\text{O}_2^{\bullet-}$ is that although both are π -type radicals, their spin and charge density distributions are not very similar. For example, the spin density distribution and charge density on the attacking atom are 73% and -0.15 e for HO_2^\bullet and 50% and -0.50 e for $\text{O}_2^{\bullet-}$, respectively. Based on the lower negative charge density and higher electron density distribution on the terminal O in HO_2^\bullet compared to $\text{O}_2^{\bullet-}$, the nature of HO_2^\bullet radical addition to $\text{C}=\text{N}$ of the nitrones can be predicted to be mostly electrophilic in nature rather than nucleophilic. Also, the presence of a low-lying first electronic excited state in HO_2^\bullet can play a major role in determining the rate of its addition to nitrones; as observed in HO_2^\bullet reactions with some olefins.⁴³

To further evaluate if a charge-transfer mechanism was playing a role in determining the rate of HO_2^\bullet addition to nitrones, the electron affinities (EA) and ionization potentials (IP) for the nitrones were calculated at the PCM/mPW1K/6-31+G(d,p)//mPW1K/6-31+G(d,p) and PCM/B3LYP/6-31+G(d,p)//B3LYP/6-31G(d) levels (Table 4). However, results show that there is no correlation between the calculated $\Delta G_{\text{rxn-2}}$ or $k_{\text{rxn-2}}$ with the theoretical EA and IP values of these nitrones (see Figure S5-S8). The same trend was observed using gas-phase energies at both levels of theory. The poor correlation between the rate constants and thermodynamic values could be due to the presence of H-bonding in the transition states that can bias the energies of the TS structures and this is further discussed below.

Unlike in the $\text{O}_2^{\bullet-}$ addition reactions,²⁵ a rationale for the trends observed for HO_2^\bullet addition favorability to some nitrones cannot be established based on calculated energies, rate constants, or electron-transfer mechanisms versus the charge density on C_2 . However, there is a direct relationship between the kinetic parameters and strong H-bond interactions between the hydroperoxyl-H and the carbonyl-O in the TS structures which improve adduct formation; although the $\text{C}_2\text{-O}_2\text{H}$ distances in all the TS structures are almost the same ($\sim 2.1 \text{ \AA}$). For example, at the mPW1K/6-31+G(d,p) level, EMAPO, DEPO, TAMPO, and CPCOMPO have strong interactions yielding $\text{OOH}\cdots\text{O}=\text{C}$ distance from 1.76 to 1.87 \AA . The other adducts have $\text{OOH}\cdots\text{NR}_2$ and $\text{OOH}\cdots\text{O}-\text{N}$ distances in the range of $2.07\text{--}2.42 \text{ \AA}$. The high $k_{\text{rxn-2}}$ value observed for EMPO cannot be rationalized in terms of strong H-bonding in the TS since the $\text{OOH}\cdots\text{O}-\text{N}$ distance observed was only 2.27 \AA , while CPCOMPO has stronger interactions yielding a $\text{OOH}\cdots\text{O}=\text{C}$ distance of 1.83 \AA , but only gave a relatively small $k_{\text{rxn-2}}$ value of $61.9 \text{ M}^{-1} \text{ s}^{-1}$. Considering that the charge densities for CPCOMPO and EMPO are quite similar ($\sim 0.04 \text{ e}$), the difference in their reactivity could not be explained in terms of charge density on the C_2 , electron affinity or the presence of H-bonding in the TS.

IV. Conclusions

The reactivity of HO_2^\bullet toward various nitrones has been assessed from theoretical free energies of reaction, bimolecular rate constants, spin and charge densities, and hydrogen-bonding interactions. The calculated rate constants are on the same order of magnitude as those observed

experimentally for spin trapping in acidic aqueous solutions (i.e., $\sim 10^2$ to $10^3 \text{ M}^{-1} \text{ s}^{-1}$). The transition state structures for HO_2^\bullet addition to the various nitrones are relatively early on the potential energy surface as evidenced by the minor distortion of the bond angles around the nitronyl-C in the transition states. However, theoretically derived kinetic and thermodynamic parameters provide poor correlations with the calculated charge densities on the nitronyl-C (C_2 , the site of radical addition) contrary to that observed for the reactivity of O_2^\bullet to nitrones; ²⁵ an indication that the HO_2^\bullet addition to nitrones is not nucleophilic in nature. Strong H-bonding interactions between the hydroperoxyl-H and the carbonyl-O in the TS for some reactions play a significant role in facilitating HO_2^\bullet addition to nitrones. This observation suggests a need for strong H-bond acceptors in the design of nitrone-based antioxidants and spin traps for efficient HO_2^\bullet scavenging in biological systems.

Supplementary Material

Refer to Web version on PubMed Central for supplementary material.

Acknowledgments

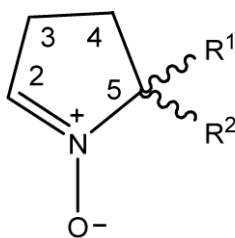
This work is supported by NIH grant HL081248. JLZ acknowledges support from the NIH grants HL38324, HL63744 and HL65608. CMH acknowledges support from the NSF-funded Environmental Molecular Science Institute (CHE-0089147). The Ohio Supercomputer Center (OSC) is acknowledged for generous computational support of this research.

References

- Halliwell B. Oxidative Stress and Disease 2001;7:1–16. Halliwell B. Drugs & Aging 2001;18:685–716. [PubMed: 11599635] Zweier JL, Talukder MAH. Cardiovascular Research 2006;70:181–190. [PubMed: 16580655] Zweier, JL.; Villamena, FA. Oxidative Stress and Cardiac Failure. Kukin, ML.; Fuster, V., editors. Futura Publishing; Armonk, N. Y.: 2003. p. 67-95.
- Sawyer DT, Chlerlato JG, Angells CT, Nannl J, EJ, Tsuchlya T. Anal. Chem 1982;1082:1720–1724.
- Behar D, Czapski G, Rabani J, Dorfman LM, Schwarz HA. J. Phys. Chem 1970;74:3209–3213.
- Czapski G, Bielski BHJ. J. Phys. Chem 1963;67:2180–2184.
- Halliwell, B.; Gutteridge, JMC. Free Radicals in Biology and Medicine. Oxford University Press; New York: 1999.
- Cheng, Z. a. L., Y. Chem. Rev 2007;107:748–766. [PubMed: 17326688]
- Zweier JL, Broderick R, Kuppusamy P, Thompson-Gorman S, Luty GA. J. Biol. Chem 1994;269:24156–62. [PubMed: 7929072]
- Zweier JL, Flaherty JT, Weisfeldt ML. Proc. Natl. Acad. U.S.A 1987;84:1404. Zweier JL, Kuppusamy P, Luty GA. Proc. Natl. Acad. U.S.A 1988;85:4046. Zweier JL, Kuppusamy P, Williams R, Rayburn BK, Smith D, Weisfeldt ML, Flaherty JT. J. Biol. Chem 1989;264:18890. [PubMed: 2553726]
- Ambrosio G, Zweier JL, Flaherty JT. J. Mol. Cell Cardiol 1991;23:1359–74. [PubMed: 1811055]
- Janzen EG. Free Radical Biol. Med 1980;4:115–154. Janzen EG. Acc. Chem. Res 1971;4:31–40. Janzen EG, Haire DL. Adv. Free Radical Chem 1990;1:253–295. Rhodes, CJ., editor. Toxicology of the Human Environment. The Critical Role of Free Radicals. Taylor and Francis; London: 2000. Rosen, GM.; Britigan, BE.; Halpern, HJ.; Pou, S. Free Radicals: Biology and Detection by Spin Trapping. Oxford University Press; New York: 1999. Villamena FA, Zweier JL. Antioxid. Redox Signaling 2004;6:619–629.
- Villamena FA, Merle JK, Hadad CM, Zweier JL. J. Phys. Chem. A 2005;109:6083–6088. [PubMed: 16833945]
- Nonogawa M, Arai T, Endo N, Pack SP, Kodaki T, Makino K. Org. Biomol. Chem 2006;4:1811–1816. [PubMed: 16633574] Zhang H, Joseph J, Vasquez-Vivar J, Karoui H, Nsanumuhire C, Martasek P, Tordo P, Kalyanaraman B. FEBS Lett 2000;473:58–62. [PubMed: 10802059]
- Breuer, E.; Aurich, HG.; Nielsen, A. Nitrones, Nitronates and Nitroxides. John Wiley and Sons; New York: 1989.

14. Floyd RA. Aging Cell 2006;5:51–57. [PubMed: 16441843] Nakae D, Kishida H, Enami T, Konishi Y, Hensley KL, Floyd RA, Kotake Y. Cancer Science 2003;94:26–31. [PubMed: 12708470] Nakae D, Uematsu F, Kishida H, Kusuoka O, Katsuda S.-i. Yoshida M, Takahashi M, Maekawa A, Denda A, Konishi Y, Kotake Y, Floyd RA. Cancer Letters (Amsterdam, Netherlands) 2004;206:1–13. Becker DA, Ley JJ, Echegoyen L, Alvarado R. J. Am. Chem. Soc 2002;124:4678. [PubMed: 11971716] Ginsberg MD, Becker DA, Busto R, Belayev A, Zhang Y, Khoutorova L, Ley JJ, Zhao W, Belayev L. Annals of Neurology 2003;54:330. [PubMed: 12953265]
15. Floyd RA, Hensley K. Ann. New York Acad. Sci 2000;899:222–237. [PubMed: 10863542]
16. Packer, L.; Cadenas, E., editors. Handbook of Synthetic Antioxidants. Marcel Dekker, Inc.; New York: 1997.
17. Fong JJ, Rhoney DH. Annals of Pharmacotherapy 2006;40:461–471. [PubMed: 16507608] Maples KR, Green AR, Floyd RA. CNS Drugs 2004;18:1071–1084. [PubMed: 15581379] Zhao Z, Cheng M, Maples KR, Ma JY, Buchan AM. Brain Research 2001;909:46–50. [PubMed: 11478919]
18. Konorev EA, Baker JE, Joseph J, Kalyanaraman B. Free Radic. Biol. Med 1993;14:127–37. [PubMed: 8425719] Pietri S, Liebgott T, Frijaville C, Tordo P, Culcasi M. Eur. J. Biochem 1998;254:256–265. [PubMed: 9660178]
19. Lapchak PA, Araujo DM, Song D, Wei J, Purdy R, Zivin JA. Stroke 2002;33:1665–1670. [PubMed: 12053009] Tosaki A, Blasig IE, Pali T, Ebert B. Free Radic. Biol. Med 1990;8:363–72. [PubMed: 2165975]
20. Finkelstein E, Rosen GM, Rauckman EJ. J. Am. Chem. Soc 1980;102:4995.
21. Boyd SL, Boyd RJ. J. Phys. Chem 1994;98:11705–11713.
22. Villamena FA, Hadad CM, Zweier JL. J. Phys. Chem. A 2005;109:1662–1674. [PubMed: 16833491]
23. Bosnjakovic A, Schlick S. Journal of Physical Chemistry B 2006;110:10720–10728. Panchenko A, Dilger H, Kerres J, Hein M, Ullrich A, Kaz T, Roduner E. Phys. Chem. Chem. Phys 2004;6:2891–2894. Yang J, Chen C, Ji H, Ma W, Zhao J. J. Phys. Chem. B 2005;109:21900–21907. [PubMed: 16853845] Yu J, Chen J, Li C, Wang X, Zhang B, Ding H. Journal of Physical Chemistry B 2004;108:2781–2783. Vakrat-Haglili Y, Weiner L, Brumfeld V, Brandis A, Salomon Y, McLlroy B, Wilson BC, Pawlak A, Rozanowska M, Sarna T, Scherz A. J. Am. Chem. Soc 2005;127:6487–6497. [PubMed: 15853357] Nam S-N, Han S-K, Kang JW, Choi H. Ultrasonics Sonochem 2003;10:39–147. Balakirev MY, Khramtsov VV. J. Org. Chem 1996;61:7263–7269. [PubMed: 11667648]
24. Chen Y-R, Chen C-L, Yeh A, Liu X, Zweier JL. Journal of Biological Chemistry 2006;281:13159–13168. [PubMed: 16531408] Dugan LL, Sensi SL, Canzoniero LMT, Handran SD, Rothman SM, Lin TS, Goldberg MP, Choi DW. J. of Neuroscience 1995;15:6377–88. Partridge RS, Monroe SM, Parks JK, Johnson K, Parker WD Jr. Eaton GR, Eaton SS. Archives of Biochemistry and Biophysics 1994;310:210–17. [PubMed: 8161207] Nohl H, Jordan W, Hegner D. FEBS Letters 1981;123:241–4. [PubMed: 6262109] Wang P, Chen H, Qin H, Sankarapandi S, Becher MW, Wong PC, Zweier JL. Proc. Natl. Acad. Sci. U S A 1998;95:4556–60. [PubMed: 9539776]
25. Villamena FA, Xia S, Merle JK, Lauricella R, Tuccio B, Hadad CM, Zweier JL. J. Am. Chem. Soc 2007;129:8177–8191. [PubMed: 17564447]
26. Frisch, MJ., et al. Gaussian, Inc.; Pittsburgh PA: 2002. Revision A.11.3 ed.
27. Labanowski, JW.; Andzelm, J. Density Functional Methods in Chemistry. Springer; New York: 1991. Parr, RG.; Yang, W. Density Functional Theory in Atoms and Molecules. Oxford University Press; New York: 1989.
28. Becke AD. Phys. Rev 1988;38:3098–3100. Lee C, Yang W, Parr RG. Phys. Rev. B 1988;37:785–789. Becke AD. J. Chem. Phys 1993;98:1372–7. Hehre, WJ.; Radom, L.; Schleyer, PV.; Pople, JA. Ab Initio Molecular Orbital Theory. John Wiley & Sons; New York: 1986.
29. Lynch BJ, Fast PL, Harris M, Truhlar DG. J. Phys. Chem. A 2000;104:4811.
30. Tomasi J, Persico M. Chem. Rev 1994;94:2027–94. Cossi M, Barone V, Cammi R, Tomasi J. Chem. Phys. Lett 1996;255:327–335. Barone V, Cossi M, Tomasi J. J. Chem. Phys 1997;107:3210. Barone V, Cossi M, Tomasi J. J. Comput. Chem 1998;19:404. Cossi M, Barone V. J. Chem. Phys 1998;109:6246.
31. Scott AP, Radom L. J. Phys. Chem 1996;100:16502–16513.
32. Lynch BJ, Truhlar DG. J. Phys. Chem. A 2001;105:2936.
33. Reed AE, Curtiss LA, Weinhold FA. Chem. Rev 1988;88:899–926.

34. Barckholtz C, Barckholtz TA, Hadad CM. *J. Phys. Chem. A* 2001;105:140–15.
35. Laidler, KJ. *Chemical Kinetics*. Harper & Row, Publishers, Inc.; New York: 1987.
36. Wigner EPZ. *Phys. Chem. Abt. B* 1932;19:203.
37. Villamena F, Dickman MH, Crist DR. *Inorg. Chem* 1998;37:1446–1453. Boeyens JCA, Kruger GJ. *Acta Cryst* 1970;B26:668. Xu YK, Chen ZW, Sun J, Liu K, Chen W, Shi W, Wang HM, Zhang XK, Liu Y. *J. Org. Chem* 2002;67:7624–7630. [PubMed: 12398482]
38. Alini S, Citterio A, Farina A, Fochi MC, Malpezzi L. *Acta Cryst* 1998;C54:1000–1003.
39. DeMatteo M, Poole JS, Shi X, Sachdeva R, Hatcher P, Hadad CM, Platz MS. *J. Am. Chem. Soc* 2005;127:7094–7109. [PubMed: 15884952]
40. Villamena FA, Rockenbauer A, Gallucci J, Velayutham M, Hadad CM, Zweier JL. *J. Org. Chem* 2004;69:7994–8004. [PubMed: 15527282]
41. Buettner GR. *Arch. Biochem. Biophys* 1993;300:535–543. [PubMed: 8434935]
42. Tsai P, Ichikawa K, Mailer C, Pou S, Halpern HJ, Robinson BH, Nielsen R, Rosen GM. *J. Org. Chem* 2003;68:7811–7817. [PubMed: 14510560]
43. Stark MS. *J. Am. Chem. Soc* 2000;122:4162–4170. Stark MS. *J. Phys Chem. A* 1997;101:8296–8301.
44. Clifford EP, Wenthold PGG, R, Lineberger WC, DePuy CH, Bierbaum VM, Ellison GB. *J. Chem. Phys* 1998;109



R ¹	R ²	Acronym
-CH ₃	-CH ₃	DMPO
-CH ₃	-CF ₃	TFMPO
-CH ₃	-C(O)NH ₂	AMPO
-CH ₃	-C(O)NHCH ₃	MAMPO
-CH ₃	-C(O)N(CH ₃) ₂	DiMAMPO
-CH ₃	-CO ₂ Et	EMPO
-CH ₃	-P(O)(OEt) ₂	DEPMPO
-CO ₂ Et	-CO ₂ Et	DEPO
-CO ₂ Et	-C(O)NHCH ₃	EMAPO
-C(O)NHCH ₃	-C(O)NHCH ₃	DiMAPO

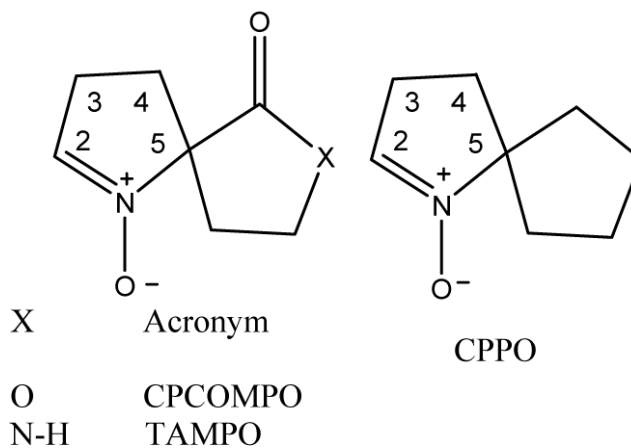
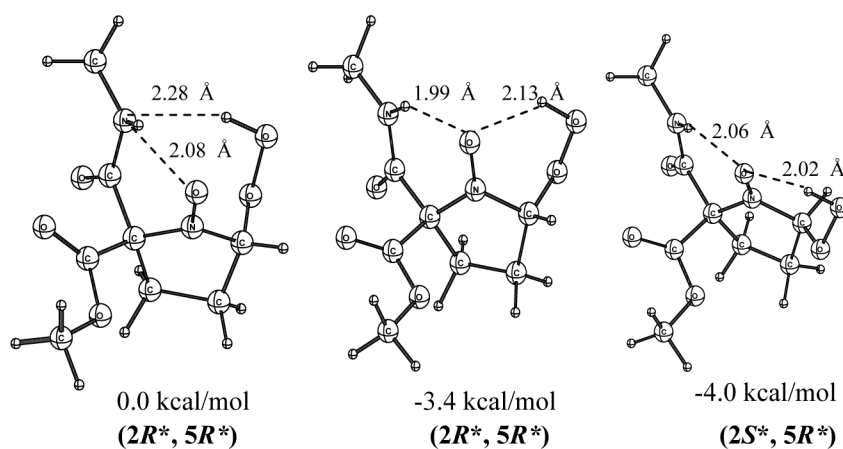


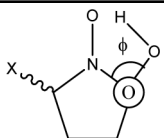
Chart 1.
DMPO-type nitrones used to theoretically investigate spin trapping of hydroperoxyl radical.

**Figure 1.**

Relative free energies in aqueous solution ($G_{298K, aq}$ in kcal/mol) of various optimized EMAPO HO_2^\bullet adducts showing strong intramolecular interactions at the PCM/B3LYP/6-31+G(d,p)//B3LYP/6-31G(d) level. Note that the preferred isomer is (*2S**, *5R**)-EMAPO- O_2H in which the hydroperoxyl moiety is *trans* to the amide group.

Table 1

Hydroperoxide nitron adduct OOCN dihedral angles for the B3LYP/6-31G(d) and mPW1K/6-31+G(d,p) (in parentheses) structures.



HO ₂ [•] Adduct	φ (°)
AMPO-cis	64.7 (66.2)
DEPMPO-trans	76.7 (77.9)
CPCOMPO-cis	56.4 (286.6)
TAMPO-cis	278.2 (270.3)
EMPO-trans	76.4 (77.3)
TFMPO-trans	77.3 (78.9)
CPPO	75.7 (76.7)
DMPO	75.9 (76.9)
DEPO	62.6 (62.3)
MAMPO-cis	64.4 (66.1)
DiMAMPO-cis	77.6 (79.4)
DiMAPO	78.4 (78.4)
EMAPO ^a	64.2 (65.7)
MSMPO-trans	78.1 (79.4)

^aWhere—OOH group is *cis* to the amide group.

Table 2

Relative enthalpies, ΔH_{298K} , and free energies, ΔG_{298K} (kcal/mol), in aqueous solution and other structural parameters for the transition state structures for HO_2^\bullet addition at the PCM/mPW1K/6-31+G(d,p)//mPW1K/6-31+G(d,p) and PCM/B3LYP/6-31+G(d,p)//B3LYP/6-31G(d) (in parentheses) levels of theory.

Structure	$\Delta H_{298K,aq}$	$\Delta G_{298K,aq}$	C...O ₂ H Å	$\langle S^2 \rangle^e$	Imaginary frequency
AMPO					
AMPO + •O ₂ H	0.0 (0.0)	0.0 (0.0)	∞	a	
AMPO...•O ₂ H	2.6 (2.8)	12.3 (13.0)	3.29 (3.24)	0.75 (0.75)	
[AMPO...•O ₂ H] [‡]	5.3 (5.1)	17.5 (17.5)	2.10 (2.10)	0.81 (0.80)	0
AMPO•O ₂ H	-18.0 (-14.6)	-5.5 (-1.6)	1.42 (1.40)	0.75 (0.75)	359i (354i)
DEPMPO					
DEPMPO + •O ₂ H	0.0 (0.0)	0.0 (0.0)	∞	a	
DEPMPO...•O ₂ H	(-3.1)	(6.7)	3.20 (3.55)	0.75 (0.75)	
[DEPMPO...•O ₂ H] [‡]	4.5 (5.1)	16.6 (17.3)	2.12 (2.10)	0.81 (0.79)	0
DEPMPO•O ₂ H	-21.0 (-17.5)	-8.6 (-4.8)	1.41 (1.41)	0.75 (0.75)	383i (416i)
DMPO					
DMPO + •O ₂ H	0.0 (0.0)	0.0 (0.0)	∞	a	
DMPO...•O ₂ H	-4.5 (-3.6)	4.8 (6.0)	3.68 (3.01)	0.75 (0.75)	
[DMPO...•O ₂ H] [‡]	4.3 (4.7)	15.8 (16.5)	2.12 (2.10)	0.81 (0.79)	0
DMPO•O ₂ H	-20.1 (-16.7)	-8.2 (-4.6)	1.41 (1.42)	0.76 (0.75)	380i (415i)
EMPO					
EMPO + •O ₂ H	0.0 (0.0)	0.0 (0.0)	∞	a	
EMPO...•O ₂ H	-4.4 (-3.8)	4.4 (5.6)	3.56 (3.48)	0.75 (0.75)	
[EMPO...•O ₂ H] [‡]	4.1 (4.5)	15.1 (15.9)	2.13 (2.10)	0.81 (0.80)	0
EMPO•O ₂ H	-20.7 (-17.5)	-9.5 (-6.2)	1.41 (1.42)	0.76 (0.75)	364i (413i)
CPCOMPO					
CPCOMPO + •O ₂ H	0.0 (0.0)	0.0 (0.0)	∞	a	
CPCOMPO...•O ₂ H	1.0 (1.2)	9.8 (10.5)	3.60 (3.67)	0.75 (0.75)	
[CPCOMPO...•O ₂ H] [‡]	4.8 (4.8)	17.0 (17.3)	2.11 (2.10)	0.83 (0.80)	0
CPCOMPO•O ₂ H	-21.7 (-17.7)	-8.7 (-4.7)	1.41 (1.42)	0.75 (0.75)	387i (323i)
TAMPO					
TAMPO + •O ₂ H	0.0 (0.0)	0.0 (0.0)	∞	a	
TAMPO...•O ₂ H	-1.5 (-1.1)	7.5 (8.6)	4.50 (4.60)	0.75 (0.75)	
[TAMPO...•O ₂ H] [‡]	2.6 (2.4)	15.0 (15.0)	2.10 (2.12)	0.83 (0.81)	0
TAMPO•O ₂ H	-21.6 (-18.2)	-8.5 (-4.9)	1.41 (1.42)	0.75 (0.75)	391i (365i)
MSMPO					
MSMPO + •O ₂ H	0.0 (0.0)	0.0 (0.0)	∞	a	
MSMPO...•O ₂ H	-3.5 (-2.7)	6.5 (7.2)	3.64 (3.51)	0.75 (0.75)	
[MSMPO...•O ₂ H] [‡]	4.8 (5.0)	16.7 (16.9)	2.14 (2.10)	0.81 (0.80)	0
MSMPO•O ₂ H	-22.6 (-19.4)	-10.2 (-7.3)	1.41 (1.41)	0.75 (0.75)	387i (439i)
TFMPO					
TFMPO + •O ₂ H	0.0 (0.0)	0.0 (0.0)	∞	a	
TFMPO...•O ₂ H	-3.6 (-2.7)	5.9 (7.2)	3.60 (3.49)	0.75 (0.75)	
[TFMPO...•O ₂ H] [‡]	4.6 (5.3)	16.1 (17.2)	2.13 (2.11)	0.81 (0.80)	0
TFMPO•O ₂ H	-21.3 (-17.8)	-9.4 (-5.8)	1.41 (1.41)	0.75 (0.75)	380i (412i)
DEPO					
DEPO + •O ₂ H	0.0 (0.0)	0.0 (0.0)	∞	a	
DEPO...•O ₂ H	0.6 (1.0)	9.8 (10.7)	3.12 (3.01)	0.75 (0.75)	
[DEPO...•O ₂ H] [‡]	2.7 (2.8)	15.1 (15.3)	2.12 (2.10)	0.82 (0.81)	0
DEPO•O ₂ H					354i (391i)

Structure	$\Delta H_{298K,aq}$	$\Delta G_{298K,aq}$	C---O ₂ H Å	$\langle S^2 \rangle^e$	Imaginary frequency
DEPO•O ₂ H	-22.4 (-18.7)	-10.1 (-6.2)	1.41 (1.42)	0.75 (0.75)	0
CPPO + •O ₂ H	0 (0.0)	0 (0.0)	∞	^a	
CPPO---O ₂ H	-3.6 (-3.8)	5.0 (6.0)	3.7 (3.23)	0.75 (0.75)	0
[CPPO•O ₂ H] [†]	4.8 (4.7)	15.7 (16.5)	2.12 (2.10)	0.80 (0.79)	374i (414i)
CPPO•O ₂ H	-19.9 (-17.1)	-8.5 (-4.8)	1.41 (1.42)	0.76 (0.75)	0
MAMPO + •O ₂ H	0.0 (0.0)	0.0 (0.0)	∞	^a	
MAMPO ---O ₂ H	3.4 (4.2)	12.8 (14.4)	3.43 (3.29)	0.75 (0.75)	0
[MAMPO•O ₂ H] [†]	6.2 (5.4)	18.5 (17.8)	2.11 (2.00)	0.81 (0.80)	358i (491i)
MAMPO•O ₂ H	-17.2 (-13.5)	-5.1 (-0.7)	1.42 (1.43)	0.76 (0.75)	0
DiMAMPO + •O ₂ H	0.0 (0.0)	0.0 (0.0)	∞	^a	
DiMAMPO ---O ₂ H	-2.3 (-2.0)	6.9 (8.9)	3.59 (3.51)	0.76 (0.75)	0
[DiMAMPO•O ₂ H] [†]	7.2 (7.5)	19.3 (19.8)	2.10 (2.10)	0.81 (0.80)	411i (423i)
DiMAMPO•O ₂ H	-21.0 (-17.5)	-8.9 (-4.7)	1.40 (1.41)	0.75 (0.75)	0
EMAPO + •O ₂ H	0.0 (0.0)	0.0 (0.0)	∞	^a	
EMAPO ---O ₂ H	4.3 (4.2)	14.5 (14.1)	3.17 (3.12)	0.75 (0.75)	0
[EMAPO•O ₂ H] [†]	6.3 (6.5)	18.8 (19.2)	2.10 (2.11)	0.81 (0.80)	367i (358i)
EMAPO•O ₂ H	-17.5 (-13.8)	-5.1 (-0.9)	1.41 (1.42)	0.76 (0.75)	0
EMAPO + •O ₂ H	0.0 (0.0)	0.0 (0.0)	∞	^a	
EMAPO ---O ₂ H	0.8 (1.4)	9.8 (10.8)	3.42 (3.68)	0.75 (0.75)	0
[EMAPO•O ₂ H] [†]	2.8 (3.2)	15.2 (15.4)	2.09 (2.11)	0.81 (0.80)	385i (368i)
EMAPO•O ₂ H	-21.1 (-17.5)	-8.0 (-4.5)	1.41 (1.42)	0.75 (0.75)	0
DiMAPO + •O ₂ H	0.0 (0.0)	0.0 (0.0)	∞	^a	
DiMAPO ---O ₂ H	-2.3 (-2.5)	9.0 (8.5)	3.20 (3.65)	0.75 (0.75)	0
[DiMAPO•O ₂ H] [†]	6.6 (5.5)	18.8 (17.9)	2.14 (2.00)	0.80 (0.80)	338i (517i)
DiMAPO•O ₂ H	-18.7 (-15.3)	-5.6 (-2.9)	1.41 (1.41)	0.76 (0.75)	0

^a At infinite separation. ^b Nitron—HO₂[•] complex. ^c Transition state. ^d Products.

^f The $\langle S^2 \rangle$ for all the nitrones is 0.00 while that of HO₂[•] is 0.75 at both levels of theory used. ^g Point group for all structures is C₁ and imaginary vibrational frequencies are in the units of cm⁻¹.

^e Values are relative energies based on single-point energy calculations with the polarizable continuum model (PCM) at the mPW1K/6-31+G(d,p) level using water as a solvent. Values in parentheses are at the PCM/B3LYP/6-31+G(d,p)/B3LYP/6-31G(d) level. Thermal and entropic corrections from the gas-phase calculations were applied with the single-point energy for the PCM level in order to get an estimated ΔH_{298K} and ΔG_{298K} in water.

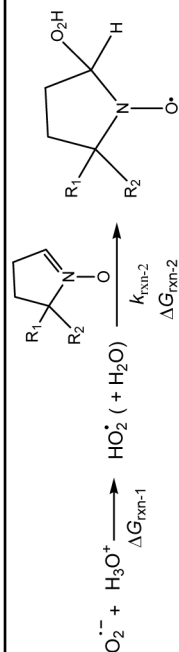
Table 3

NPA Charges and Spin Densities (Populations) of Transition States for the formation of various Hydroperoxyl Adducts at the B3LYP/6-31+G**/B3LYP/6-31G* level, in units of electrons.

	N	O _{nitroxyl}	β-O	γ-O
AMPO	0.02, 0.17	-0.50, 0.28	-0.26, 0.53	-0.41, 0.18
DEPMPO	0.02, 0.19	-0.51, 0.27	-0.26, 0.53	-0.42, 0.16
DMPO	0.04, 0.18	-0.50, 0.28	-0.27, 0.53	-0.43, 0.15
EMPO	0.04, 0.18	-0.49, 0.29	-0.27, 0.53	-0.43, 0.16
CPCOMPO	0.04, 0.16	-0.47, 0.29	-0.28, 0.54	-0.40, 0.19
TAMPO	0.04, 0.18	-0.47, 0.31	-0.25, 0.53	-0.43, 0.17
MSMPO	0.01, 0.18	-0.47, 0.31	-0.27, 0.52	-0.42, 0.16
TFMPO	0.03, 0.17	-0.48, 0.29	-0.26, 0.54	-0.42, 0.17
DEPO	0.03, 0.15	-0.44, 0.33	-0.28, 0.51	-0.41, 0.19
CPPO	0.04, 0.19	-0.51, 0.27	-0.26, 0.53	-0.43, 0.16
MSMPO	0.01, 0.18	-0.47, 0.31	-0.27, 0.52	-0.42, 0.16
MAMPO	0.01, 0.22	-0.46, 0.37	-0.29, 0.44	-0.44, 0.13
DiMAMPO	0.03, 0.19	-0.51, 0.26	-0.25, 0.55	-0.43, 0.16
DiMAPO	0.03, 0.26	-0.47, 0.36	-0.28, 0.43	-0.44, 0.11
EMAPO cis	0.03, 0.16	-0.49, 0.28	-0.26, 0.53	-0.40, 0.19
EMAPO trans	0.02, 0.17	-0.49, 0.28	-0.26, 0.53	-0.40, 0.20

Table 4

Aqueous phase charge densities of the nitronyl-C (C_2), electron affinities, ionization potentials (eV) of the nitrones, rate constants (k , $M^{-1} s^{-1}$), and free energies of reaction^a (ΔG_{rxn} , kcal/mol) for the formation of hydroperoxyl adducts at the PCM/mPW1K/6-31+G(d,p) and PCM/B3LYP/6-31+G(d,p) levels of theory.



Entry	PCM/mPW1K/6-31+G(d,p)//mPW1K/6-31+G(d,p)					PCM/B3LYP/6-31+G(d,p)//B3LYP/6-31G(d)				
	C_2 Charge (e)	EA (eV) ^d	IP (eV) ^e	k_{rxn-2}	ΔG_{rxn-2}	C_2 Charge (e)	EA (eV) ^d	IP (eV)	k_{rxn-2}	ΔG_{rxn-2}
AMPO	0.054	-1.90 (0.10) ^f	6.27 (8.22) ^f	26.6	-5.5	0.060	-1.91 (0.68)	6.33 (8.01)	25.0	-1.6
DEPMPO	0.038	-1.74 (0.32)	6.22 (7.78)	125.8	-8.6	0.043	-1.63 (0.61)	6.26 (7.59)	71.7	-4.8
CPCOMPO	0.04	-1.92 (0.15)	6.33 (8.27)	61.9	-8.7	0.045	-2.32 (0.04)	6.37 (8.06)	39.2	-4.7
TAMPO	0.034	-1.69 (0.39)	6.18 (7.98)	1936.5	-8.5	0.038	-1.64 (1.11)	6.21 (7.75)	1835.0	-4.9
EMPO	0.035	-1.73 (0.37)	6.22 (8.02)	1528.4	-9.5	0.040	-1.77 (0.86)	6.25 (7.81)	411.9	-6.2
TFMPO	0.038	-1.88 (0.29)	6.33 (8.36)	276.0	-9.4	0.043	-1.91 (0.96)	6.39 (8.13)	48.3	-5.8
CPPO	0.015	-1.55 (0.73)	6.04 (7.94)	1140.6	-8.5	0.024	-1.63 (1.29)	6.04 (7.72)	294.2	-4.8
DMPO	0.013	-1.54 (0.73)	6.06 (7.98)	1002.3	-8.2	0.019	-1.56 (1.38)	6.09 (7.79)	285.5	-4.6
DEPO	0.039	-1.85 (0.25)	6.33 (7.96)	2982.3	-10.1	0.043	-2.87 (-0.81)	6.36 (7.71)	2073.0	-6.2
MSMPO	0.047	-3.14 (-1.47)	6.34 (8.08)	105.9	-10.2	0.053	-3.44 (-0.86)	6.37 (7.88)	73.5	-7.3
MAmPO	0.056	-1.92 (0.12)	5.74 (7.65)	4.6	-5.1	0.060	-1.93 (0.68)	5.95 (7.58)	17.7	-0.7
DiMAmPO	0.026	-0.67 (0.73)	6.08 (7.64)	1.3	-8.9	0.030	-1.53 (0.72)	6.08 (7.35)	0.6	-4.7
DiMAPO	0.092	-2.20 (-0.38)	6.037 (8.15)	5.8	-5.6	0.098	-2.21 (0.11)	6.36 (7.87)	32.6	-2.9
EMAPO (cis) ^b	0.069	-2.08 (-0.08)	5.89 (7.47)	3.0	-5.1	0.073	-2.10 (0.46)	6.08 (7.38)	1.5	-0.9
EMAPO (trans) ^c	0.069	n/a	n/a	1359.0	-8.0	0.073	n/a	n/a	876.2	-4.5
HOO [•]	n/a	-4.02 (-0.80) ^g	8.33 (11.98)	n/a	n/a	n/a	-4.22 (0.29)	8.47 (11.88)	n/a	n/a

^a $\Delta G_{rxn-1} = -41.1$ kcal/mol at the PCM/mPW1K/6-31+G**//mPW1K/6-31+G** or -40.5 kcal/mol at the PCM/B3LYP/6-31+G**//B3LYP/6-31G*. Energetics are derived from the hydroperoxyl radical adduct structures resulting from the 10% displacement of their respective TS structure.

^b Adduct has the hydroperoxyl moiety cis to the amide group.

^c Adduct has the hydroperoxyl moiety trans to the amide group (or cis to the ester group).

^d Calculated as $EA = \Delta H_{298K}(\text{radical anion}) - \Delta H_{298K}(\text{neutral})$

^e Calculated as $IP = \Delta H_{298K}(\text{radical cation}) - \Delta H_{298K}(\text{neutral})$.

^f Values in parentheses are in gas phase.

^g Calculated EA and IP for HO₂[•] are defined as $EA = \Delta H_{298K}(\text{HO}_2^{\cdot-}) - \Delta H_{298K}(\text{HO}_2^{\cdot+})$ and $IP = \Delta H_{298K}(\text{HO}_2^{\cdot+}) - \Delta H_{298K}(\text{HO}_2^{\cdot-})$. The absolute EA for HO₂[•] in the gas phase is 0.80 eV at the mPW1K/6-31+G** level ($EA_{\text{expt}} = 1.089 \pm 0.006$ eV)⁴⁴.